EPJ Web of Conferences **44**, 04004 (2013)
DOI: 10.1051/epjconf/20134404004

Modeling of Kr-Xe discharge of excimer lamp

S.Bendella, B.Larouci and A.Belasri
Laboratory of Plasma physics, Materials conducting and their Applications
Department of Physics U.S.T.O.MB El M'NAOUER B.P1505Oran(ALGERIA)

Abstract: This paper reports the numerical simulation of Dielectric Barrier Discharge (DBD) for Kr-Xe excilamp. The model of the discharge consists of three main modules: a plasma chemistry module, a circuit module and a Boltzmann equation module. The results predict the optimal operating conditions and describe the electrical and chemical properties of the KrXe* excimer lamp.

1 Introduction

The discharge lamps sources of UV and VUV radiation are mainly lamps with mercury vapour [1-3]. The standards of environmental protection becoming increasingly requiring, the manufacturers of lamps are concerned with problems generated by the presence of mercury in their applications. The objective is to consider the operation of tubes with discharges in the presence of rare gas or of mixture of rare gases, without mercury. The excimer lamp can substitute mercury lights [4-5]. If one compares them with conventional lamps UV, the excimer lamp offer performances which improve the use of radiation UV and open new prospects in industry [6-7], the chemistry of preparation [8-12]. Additionally, applications of excimer lamps in photomedical research seem to have great potentials, for example, with respect to the phototherapy of psoriasis (XeCl*, 308 nm), or to wavelength-selective phototoxicity testing of drugs [13-14]. The XeCl* excimer lamp may be a cheap alternative to the 308-nm laser [15] in the treatment of psoriasis and several other inflammatory diseases. Their monochromatic spectrum and the possibility of selecting specific wavelengths allow a concentration of the photo process. Moreover, there is not any effect of parasitic heat, excimer lamp UV not producing any infra-red radiation in their spectrum. Excimer lamp can be pumped by pulsed [16-21] or dc longitudinal discharges [22], by pre-ionized pulsed transverse discharges [23], by microwave discharges [24] or by dielectric barrier discharges [25-26].

2 Physical model

In the positive column, the plasma is homogeneous and represented by a variable resistance whose conductivity is proportional to the electron density. The time dependence of the resistance $R_g(t)$ is obtained by:

$$R_g(t) = \frac{d_{pl}}{Aen_e(t)\mu_e(t)}$$

Where e, $n_e(t)$ and $\mu_e(t)$ are the electron charge, the time dependent electron density and mobility respectively. A represents the electrode area and d_{pl} is the plasma length.
The electronic density is obtained by resolving the continuity equation:

$$\frac{dn_e(t)}{dt} = S(t)$$

Where S(t) is the source term in the positive column, which takes into account the electron creation and loss. The electron continuity equation is simultaneously resolved with the kinetic equations describing the time evolution of specie concentrations. The kinetic scheme employed is reported in Table I.

TABLE I. List of reaction processes and their rate coefficients used in the present work (*Te* is the electron temperature).

Processes	Rate coefficients	References
Excitation		
$e + Kr \rightarrow Kr^* + e$	k_1 (tabulated values)	[27]
$e + Xe \rightarrow Xe^* + e$	k_2 (tabulated values)	[27]
$e + Kr^* \rightarrow Kr + e$	$k_9 = 3 \times 10^{-9}\ cm^3S^{-1}$	[28]
Direct ionization		
$e + Kr \rightarrow Kr^+ + 2^e$	k3 (tabulated values)	[27]
$e + Xe \rightarrow Xe^+ + 2\ e$	k4 (tabulated values)	[27]
Stepwise ionization		
$e + Xe^* \rightarrow Xe^+ + 2\ e$	k_5 (tabulated values)	[27]
$e + Kr^* \rightarrow Kr^+ + 2^e$	$k_6 = 4{,}8 \times 10^{-8}\ cm^3S^{-1}$	[34]
Penning ionization		
$2Kr_2^* \rightarrow Kr_2^+ + 2Kr + e$	$k_7 = 1{,}1\times10^{-9}\ cm^3S^{-1}$	[28,30]
$2Kr^* \rightarrow Kr^+ + Kr + e$	$k_8 = 1{,}1\times10^{-9}\ cm^3S^{-1}$	[28,30]
Formation of dimer ions		
$Kr^+ + Kr + Kr \rightarrow Kr^+_2 + Kr$	$k_{10} = 2{,}3 \times 10^{-31}\ cm^6\ S^{-1}$	[31]
$Xe^+ + 2Kr \rightarrow KrXe^+ + Kr$	$k_{11} = 2 \times 10^{-32}\ cm^6\ S^{-1}$	[32]
$Kr_2^+ + Xe \rightarrow Xe^+ + 2Kr$	$k_{12} = 2\times 10^{-10}\ cm^3S^{-1}$	[32]
$Kr_2^+ + e \rightarrow Kr^+ + Kr + e$	$k_{13} = 1\times 10^{-7}\ cm^3S^{-1}$	[33]
Electron-ion recombinaison		
$Xe_2^+ + e \rightarrow Xe^{**} + Xe$	$k_{14} = 2\times 10^{-7}\ Te^{-0,5}\ cm^3s^{-1}$	[38]
$KrXe^+ + e \rightarrow Xe^* + Kr$	$k_{15} = 1{,}6\times10^6(300/T_e)^{0,72}$	[32]
$Xe^+ + Xe + Kr \rightarrow Xe_2^* + Kr$	$k_{16} = 2\times10^{-31}\ cm^6\ S^{-1}$	[34]
$Kr_2^+ + e \rightarrow Kr^*(^3p_2) + Kr$	$k_{17} = 3\times10^{-7}\ cm^3S^{-1}$	[33]
ion-atom Reactions		
$KrXe^+ + Xe \rightarrow Xe_2^+ + Kr$	$k_{18} = 2\times10^{-10}\ cm^3S^{-1}$	[32]
$Xe^+ + 2Kr \rightarrow KrXe^+ + Kr$	$k_{19} = 2\times10^{-32}\ cm^6\ S^{-1}$	[32]
Kinetics of the neutres		

$Xe^* + Xe + Kr \rightarrow Xe_2^* + Kr$	$k_{20} = 5{,}4 \times 10^{-32}\ cm^6\ S^{-1}$	[29,32]
$Xe^* + Xe + Xe \rightarrow Xe_2^* + Xe$	$k_{21} = 5 \times 10^{-32}\ cm^6\ S^{-1}$	[29]
$Kr^* + Kr + Kr \rightarrow Kr^*_2 + Kr$	$k_{22} = 2 \times 10^{-32}\ cm^6\ S^{-1}$	[29]
$Kr^* + Kr + Xe \rightarrow Kr^*_2 + Xe$	$k_{23} = 2 \times 10^{-32}\ cm^6\ S^{-1}$	[29]
$Xe^* + 2Kr \rightarrow KrXe^* + Kr$	$k_{24} = 3 \times 10^{-32}\ cm^6\ S^{-1}$	[32,34]
$Kr_2^* + Xe \rightarrow Xe^* + 2Kr$	$k_{25} = 4{,}4 \times 10^{-10}\ cm^3 S^{-1}$	[32,34]
$KrXe^* + Xe \rightarrow Xe_2^* + Kr$	$k_{26} = 1 \times 10^{-10}\ cm^3 S^{-1}$	[32,28]
$Kr^* + Xe \rightarrow Kr + Xe^*$	$k_{27} = 1{,}6 \times 10^{-10}\ cm^3 S^{-1}$	[37,34]
$Kr_2^* + e \rightarrow Kr^* + Kr + e$	$k_{28} = 1.9 \times 10^{-9}\ cm^3 S^{-1}$	[33]
Spontaneous Emissions		
$Xe_2^* \rightarrow 2\,Xe + h\nu_{172}$	$k_{29} = 1{,}82 \times 10^8\ S^{-1}$	[36]
$Kr^*_2 \rightarrow 2Kr + h\nu_{148}$	$k_{30} = 3 \times 10^8\ S^{-1}$	[32]
$KrXe^* \rightarrow Kr + Xe + h\nu_{154}$	$k_{31} = 2 \times 10^8\ S^{-1}$	[32]

3 Results and discussions

In this work, the discharge was filled with a10% of Xe in the Kr mixture with a total pressure of p_r=400 Torr, a gas temperature T_g = 300°K, electrode areas A= 1 cm^2, a gap length d=0,5 cm. In order to have homogeneous plasma, we introduced a preionization density. The preionization density used is equal to 10^9 cm^{-3}, the dielectric capacitance C_{diel} is 0.23 nF and an applied voltage of V_a = 3kV.

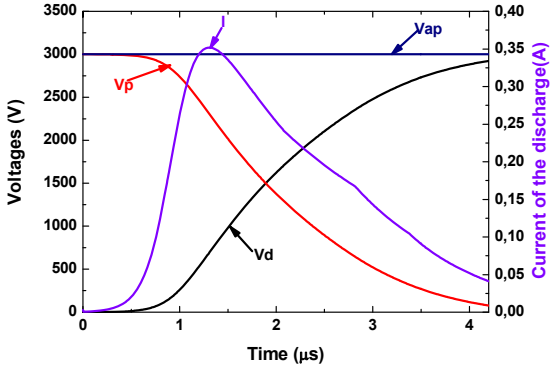

Fig1. Time variation of the current I, the voltage across the dielectric Vd, the voltage Vp of the gas, and the applied voltage Vap.

In Figure 1 we plot the time variation of the discharge current I, the voltage across the dielectric Vd, the voltage Vp of the gas, and the applied voltage Vap for an applied voltage of 3000V at a pressure of 400 torr. The voltage Vd starts to increase by the effect of dielectric loading to a peak corresponding to the applied voltage, while the discharge voltage Vp decreases rapidly after the breakdown of the gas.

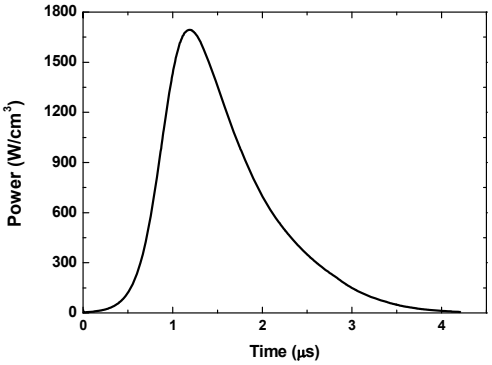

Fig2. Time evolution of the power deposited by the electrons in the plasma.

The time evolution of the power deposited by the electrons in the plasma during the discharge is plotted in figure 2. Note the power profile is identical to that of the pulse discharge. The pulse duration is 4.3µs and peak power reaches 1700 W/cm3 to 1.2µs. This value corresponds to the power of a few thousandth of joules total energy dissipated in the plasma, this energy is sufficient to sustain a discharge pulse. To observe the evolution of excited species and ionized, we plotted on Figure 3, 4 and 5 densities of charged particles, neutrals, excited and photons for the gas mixture KrXe-10%. We considered 31 collisional processes for 14 different species, this reaction system is sufficient to describe the properties of electric discharge.

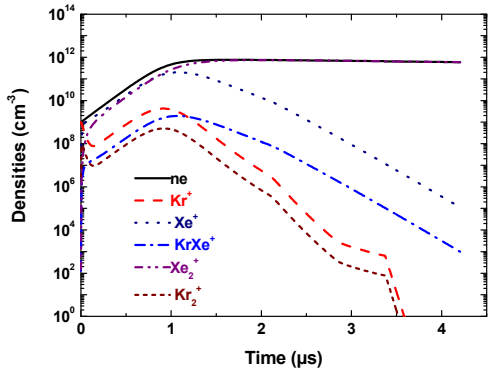

Fig3. Time variation of the plasma electron number density *ne* and ionized species concentrations.

Figure 3 shows the time evolution of the electron density and the density of ionized species in the mixture KrXe-10%. After ignition of the discharge, the rapid growth of the concentration of electrons and ionized species concentrations is noted. The dominant ions in the positive column are Xe^+ and $Xe2^+$.

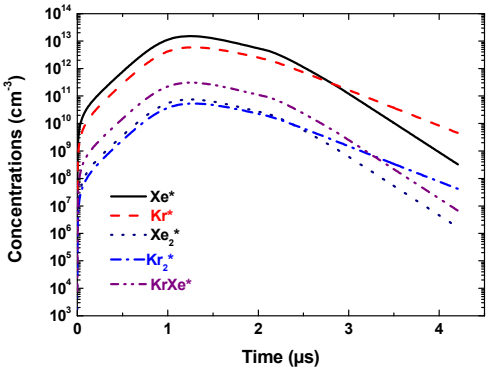

Fig4. Time variation of the plasma excited species concentrations

Variations in the time of atoms and molecules excited Xe* Kr*, Xe_2* and Kr_2* et KrXe* are plotted in Figure 4. The metastable state Xe* reaches a maximum value of 10^{13} cm^{-3} and then decreases slowly during the discharge pulse, while the concentration of Kr* reaches a maximum of 5 × 10^{12} cm^{-3} and decreases than Xe*. However, the temporal variation of the concentration of Kr_2* is almost identical to that of Kr* with a maximum value of 2 × 10^{10} cm^{-3}.

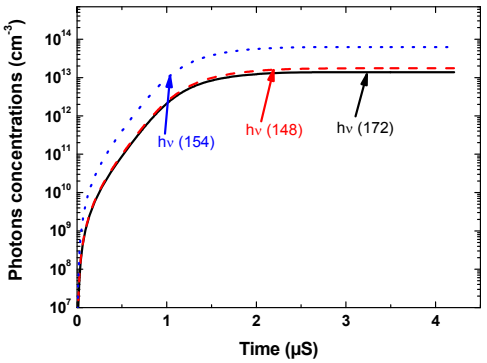

Figure5. Time variation of photon density in plasma

According to the operating conditions of a dielectric barrier discharge for excimer lamp, VUV radiation is generated by the radiative decay of the excited states of xenon: Xe_2* level (172 nm), the level Kr_2* (148 nm) and level KrXe* (154 nm). Time variation in species photonic: hv (172 nm), hv (148 nm) and hv (154 nm) were shown in Figure 5.

4 Conclusions

The present work represents a study of the kinetics for a Kr-Xe lamp pumped by a Dielectric Barrier Discharge DBD at high pressure. This study is executed by a zero-dimensional model where there is a coupling between plasma, heavy-species kinetics and the external circuit. The plasma generated by a Dielectric Barrier Discharge has been represented by one resistor. The kinetics of the heavy species has been represented using a set of reactions in order to take into account the electric behavior of the discharge. From the developed zero-dimensional model, we have analyzed the kinetics of the Kr-Xe excimer lamp mixture and the electrical discharge characteristics. The present analysis and discussions will be helpful for the design of commercial Kr/Xe lamp cells.

5 References

1. G.Zissis, P.Bénétruy and I.Bernat, Physical Review A, **Vol45**.N°2. 1135 (1992)
2. K.Charrada, G.Zissis and M.Aubes, J.Phys.D:Appl.phys.**29** 2432 (1996)
3. L.P.Bakker and G.M.W.Kroesen, Journal of Applied physics. **Vol90**. N°8 3720 (2001)
4. U.Kogelschatz, Pure Appl.Chem. **Vol 62** 1667 (1990)
5. U.Kogelschatz, B.Elliasson and W.Egli, Pure Appl. Chem. **Vol71**, N°10 1819 (1999)
6. U.Kogelschatz, B.Eliasson and W.Egli, J.Phys.IV **7** 47 (1997)
7. E.A.Sosnin, S.M.Avdeev, E.A.Kuznetzova and L.V.Lavrenteeva, Instruments and experimental techniques, **Vol48**, N°5 663 (2005)
8. B.Elliasson and U.Kogelschatz, IEEE trans. Plasma Sci. **Vol19**. 1063 (1991)
9. F.Massines, C.Mayoux, R.Messaoudi, A.Rabehi and P.Segur, In Proc. *Int. Conf. Gas Discharges and their Applications*, Swansee, UK. 730 (1992)
10. M.Laroussi, IEEE Trans. Plasma Sci. **Vol24**. 1188 (1996)
11. H.W.Hermann, I.Henins, J.Parkand G.S.Selwyn, Phys.Plasmas. **Vol6** N°5. 2284 (1999)
12. M.Laroussi, I.Alexeff and W.Kang, IEEE.Trans. Plasma Sci. **Vol28** 184 (2000)
13. K. Ko¨llner, M.B. Wimmershoff, C. Hintz, M. Landthaler and U. Hohenleutner, British Journal of Dermatology **152** 750 (2005)
14. Oppenländer, Eur. Photochem. Assoc. Newslett. Nr. **50**, S 2 (1994)
15. Spann, C. T., Barbagallo, J., and Weinberg, Cutis, **68** 351 (2001)
16. R.P.Mildren, R.J.Carman and I.S.Falconer, J.Phys D: Appl.Phys**.34** 3378 (2001)
17. R.P.Mildren, R.J.Carman and I.S.Falconer, ieee transaction on plasma science, **vol30** n°1 192 (**2002**)
18. R.P.Mildren and R.J.Carman, IEEE Transactions on Plasma Science **Vol 30** n°1 (2002)
19. R.J.Carman and R.P.Mildren, J.Phys.D: Appl.Phys.**36** 19 (2003)
20. EA. Bogdanov and all, J.Phys.D :Appl.Phys **37** 2987 (2004)
21. R.J.Carman, R.P.Mildren, B.K.Ward and D.M.Kane, J.Phys.D: Appl.Phys.**37** 2399 (2004)
22. D.Winske and M.E.Jones, IEEE Transactions on Plasma Science **Vol 22** n°4 (1994)
23. S.Bollanti and all, IEEE. Trans. Plasma Sci, **Vol 27** 211 (1999)
24. J.D.Ametepe, J.Diggs and D.M.Manos, Journal of applied physics, **Vol 85**, N° 11 7505 (1999)
25. M.V.Erofeev and V.F.Tarasenko, J.Phys.D: Appl.Phys. **39** 3609 (2006)
26. U.Kogelschatz, B.Eliasson and W.Egli, J.Phys.IV **7** 47 (1997)
27. BOLSIG. KINEMA. Software. http://www.siglo-kinema.com
28. G. N. Zvereva, ISSN 0030-400X, Optics and Spectroscopy, 2006, **Vol. 100**, No. 6, pp. 818–824 (2006).
29. Jun-Seok Oh, and Kunihide Tachibana, **102**, 073301 (2007).
30. G. N. Zvereva, Optics and Spectroscopy **Vol. 108**, No. 1, pp. 4–11 (2010).
31. *A. K. Bhattacharya,* cataphoretic segregation processes in krypton-xenon mixture, Applied Physics Letters, **Vol IS**, Number II, (1969).
32. G. N. Zvereva, Optics and Spectroscopy, **Vol. 94**, No. 2, 2003, pp. 191–198. Translated from Optika i Spektroskopiya, Vol. 94, No. 2, pp. 220–227, (2003).
33. Hyun Sook Bae and Ki-Woong Whang, Journal of the Korean Physical Society, **Vol. 53**, No. 2, pp. 624_630 August (2008).
34. M. Boichenko and S. I. Yakovlenko, Laser Physics, **Vol. 14**, No. 1, pp. 1–14, (2004).
35. Hyun Sook Bae and Ki-Woong Whang, Journal of the Korean Physical Society, **Vol. 53**, No. 2, pp. 624_630 August (2008).
36. J. W. Keto, R. E. Gleason, and G. K. Walters, Phys. Rev. Lett. **33**, 1365(1974).
37. N N Guivan, J Janˇca, A Brablec, P S´tahel, P Slavicek and L L Shimon, J. Phys. D: Appl. Phys. **38** 3188–3193 (2005).
38. J. Meunier, Ph. Belenguer, J.P. Boeuf, J. Appl. Phys. **78**, 731, (1995).